Simulation of Drying Uniformity inside Hybrid Solar Biomass Dryer using ANSYS CFX

Jackis Aukah., Mutuku Muvengei., Hiram Ndiritu and C. Onyango

***Abstract*—** In a hybrid solar biomass system, a combined solar radiation with biomass heating source is employed in order to have a double heating of the drying air. The dryer is of tunnel type where the collector and the drying tunnel are fabricated as one unit. The trays in the drying chamber are arranged horizontally at the same level slightly above the absorber plate. Solar hybrid dryers present a viable option for drying of maize since continuous drying can be achieved. However, non-uniform drying of the product may occur in the drying chamber due to poor air flow distribution. The aim of this study was to develop a mathematical model for predicting the drying uniformity within the drying chamber of a hybrid solar biomass tunnel dryer. The model consists of the full set of partial differential equations that describe the conservation of mass, momentum and heat inside the dryer. The standard k-ε model was used to describe turbulence in addition to the governing conservation equations. The simulation was done using ANSYS CFX which is a general purpose Computational Fluid Dynamics (CFD) package. The simulated air flow pattern and temperature distribution on the horizontal and vertical planes in the drying chamber was analyzed and the result revealed spatial homogeneity of drying air condition. However the velocity profile was higher at the inlet and outlet. The increase of the velocity at the exhaust stack was due to the reduction of flow cross-section area as well as chimney effect.

***Keywords*—** ANSYS CFX, Drying uniformity, Hybrid solar biomass dryer, Simulation,

I. Introduction

DRYING is an essential process used all over the world for the preservation of farm produce. It helps in reducing the water activity of the produce to a level below which deterioration does not occur for a definite duration [1]. The drying process helps to achieve better product quality, longer safe storage period and reduction in post-harvest losses. The reduction in post-harvest losses ensures more food availability for growing world population [2]. Various drying methods are employed to dry different types of food produce. Natural sun drying is the oldest method of food preservation. However, it has several drawbacks, such as the difficulty to control the rate of drying, insect infestation and microbial contamination. Replacing natural sun drying by conventional dryers or by solar dryers can significantly reduce these drawbacks and the losses caused by them. Nevertheless, the drying air characteristics in solar dryers depend on ambient conditions, which can reduce the quality of the final product.

Conventional or mechanized drying requires higher operational costs and such units are beyond the reach of farmers with limited product volume and financial resources. Moreover, the increasing rate of fuel consumption in agriculture has made it necessary, not only to save energy by intensifying the drying process, improving designs and using renewable energy sources for drying processes [3]. Solar drying has been used for a very long time and it is an effective method to preserve farm produce. Solar dryers depend on the intensity of the solar radiation to heat up the air and effect drying, but the drying process is interrupted during cloudy, rainy seasons and at night. Therefore, integration of an auxiliary heating source is essential for solar dryers to operate continuously. In this context, hybrid solar dryers present an interesting solution [4]. In hybrid solar-drying the characteristics of the drying air can be controlled, hence improving the quality of dried products and reducing the drying costs. The key factors considered in the development of solar-assisted drying systems for agricultural produce are compact collector design, high efficiency, integrated storage, and long-life drying system. In hybrid dryers, the drying process is not so dependent on the incident solar radiation, since an auxiliary source of energy can be used to maintain uniform drying conditions.

In tropical and subtropical countries, a large proportion of grain (such as maize) is harvested and stored under hot and humid conditions, and most farmers lack proper knowledge, equipment and methods of drying grains [5]. Subsequently, grain is stored while still relatively moist and warm environment. However both warmth and high moisture contents can result in rapid deterioration of the grains and promote the growth of microorganisms (e.g. fungi and bacteria) and insects in the grains [6]. To maintain high quality maize during storage, maize should be protected from extreme weather (including relative humidity and temperature), growth of microorganisms, and insects [7]. Tuite and Foster [8] also reported that insects in grain enhance mould development because they increase moisture content and temperature, and open areas of the grain for attack. Fungal growth in maize is facilitated by hot and humid conditions. It has been reported in

Aukah J., Kenya Industrial Research and Development Institute, KIRDI (corresponding author to provide phone: +2540722228281; e-mail: aukajakiz@gmail.com).

Muvengei M.. Author, Department of Mechanical Engineering, JKUAT (e-mail: author@eng. jkuat.ac.ke).

Ndiritu H., Department of Mechanical Engineering, JKUAT (e-mail: authors@eng.jkuat.ac.ke)

Onyango C., Kenya Industrial Research and Development Institute, KIRDI (e-mail: author@eng.jkuat.ac.ke)

 ISSN: 2079-6226

various studies that fungal infestation in maize results in colour changes, decrease in nutritional values, and reduction of overall quality of the maize [9].

Jackis et al. [10] designed a hybrid solar biomass tunnel dryer (HSBD) to address the challenges faced by rural maize farmers in Kenya. This dryer combines the advantages of solar- and biomass-powered drying systems. A biomass heating system was chosen for auxiliary heating source since biomass is locally available in rural areas and is often the cheapest source of energy. Solar tunnel dryers have previously been used with success for drying grain with considerable reduction in grain losses, and they offer numerous advantages such as protection of drying material from contamination, quick and uniform drying, and superior milling and germination qualities. One of the most important aspects of the drying technology, especially for industrial processes, is modeling of the drying processes. The purpose of modeling is to allow engineers to choose the most appropriate method of drying a given product, as well as suitable operating conditions. Full-scale experiments for different products and system configurations are sometimes costly and not feasible. Therefore, prediction of drying kinetics of specific crops under various conditions is very useful in design and optimization of dryers. The aim of this study was to develop a mathematical model for predicting uniform airflow distribution throughout the drying chamber using CFD simulation. Simulation was done in several horizontal planes inside the drying chamber to determine the tray position with better airflow distribution in the HSBD.

II. Methods and simulation

A. *Description of Experimental setup*

The developed HSBD consists of three main parts namely; solar collector, drying chamber and biomass auxiliary heating chamber all fabricated as one single unit (Fig. 1).

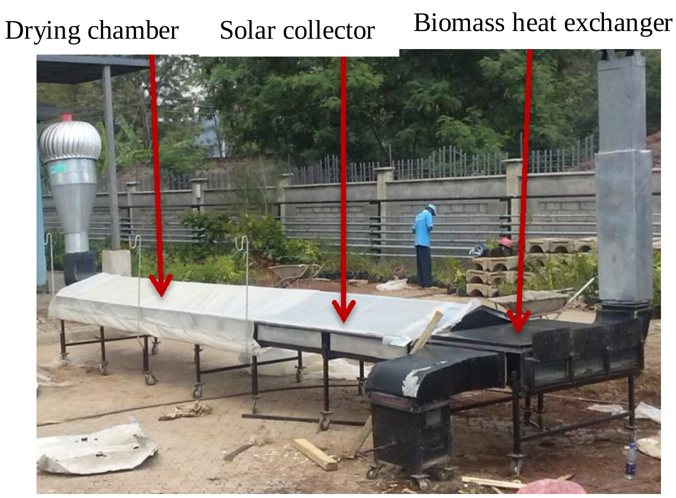

Fig. 1: Assembled biomass stove heat exchanger system

Each part of the dryer was designed to be detached and assembled without difficulty for shifting purposes from one place to another and also mounted on caster wheels for easy mobility. The top surfaces of the collector and drying chamber was designed in triangular shape and both chambers covered with UV-stabilized plastic sheet. Black paint was used to help the plate to collect solar radiation and convert it into heat energy and transfer the heat to the air surrounding the plate during the day when sufficient solar radiation is available. The main tunnel dryer frame was made of mild steel square hollow tube and angle lines with pieces of hardwood arranged at the bottom part to act as insulation material to reduce heat loss from the bottom of the dryer. The pieces of the hardwood at the bottom were covered with alluminium painted galvanized iron sheet (GI) to reflect energy incident on the surface. Similarly, the side walls of the tunnel chamber were made of alluminium coated GI sheet riveted on the main frame.

The dryer was designed to dry approximately 15 kg (wet basis) of maize in one tray per batch. The drying chamber of the dryer can accommodate six trays made of perforated plastic mesh fixed on alluminium angle line frame as shown in Fig. 2. The trays are arranged horizontally at a higher level above the absorber plate to allow for smooth flow of drying air on top and beneath the maize preventing the need to turn it during drying as shown in Fig. 3.

Fig. 2: Tray details

Fig. 3: Tray arrangement in the drying tunnel of the HSBD

To reduce its dependence on solar radiation for operation and to improve the quality of drying, a biomass stove - heat exchanger system was incorporated in this dryer, thus converting it to a hybrid dryer. The biomass stove-heat exchanger system as shown in Fig. 4 was designed mainly to compliment the solar energy supply to the dryer, and to sustain the drying process during cloudy weather. In addition it can also be used to extend the period of drying beyond sunshine hours and during night as well, while drying high value addition crops.

ISSN: 2079-6226

Fig. 4: Assembled biomass stove heat exchanger system

The whole dryer system was designed to be disassembled into small parts during transportation and also supported on a base frame mounted on castor wheels for easy mobility of the dryer as shown in Fig. 1. The tunnel dryer was also fitted with a turbo ventilator to provide the required air flow over the products to be dried. The turbo ventilator depends entirely on the wind effect and the exhaust air from the drying tunnel to operate. The centrifugal force caused by the spinning vanes creates a region of low pressure area which draws in ambient through the inlet door located at the other end of the dryer and exits hot air from the dryer.

B. Mathematical model

The differential equations which are solved express a principle of conservation and are known as continuity, momentum and energy equations. To discretize the governing equations the software ANSYS CFX makes use of an element-based finite volume method, which firstly involves discretizing the spatial domain using a mesh (Figure 2). The mesh is used to construct finite volumes, which are used to conserve relevant quantities such as mass, momentum, and energy. All solution variables and fluid properties are stored at the nodes (mesh vertices). A control volume is constructed around each mesh node and these equations are integrated over each control volume (ANSYS CFX, 2006). [11], [12]

The mass, momentum and energy equations are given in general form as:

- Mass conservation equation:

$$\frac{\partial \rho}{\partial t} + \nabla \bullet (\rho U) = 0 \quad (1)$$

- Momentum conservation equation:

$$\frac{\partial (\rho U)}{\partial t} + \nabla \bullet (\rho U \otimes U) = -\nabla p + \nabla \bullet \tau + S_M \quad (2)$$

Where is the stress tensor given by:

$$\tau = \mu \left[\nabla U + (\nabla U)^T - \frac{2}{3} \delta \nabla \bullet U \right]$$

 ISSN: 2079-6226

- Energy conservation equation:

$$\frac{\partial(\rho h_{tot})}{\partial t}-\frac{\partial p}{\partial t}+\nabla\bullet(\rho U h_{tot})=\nabla\bullet(\lambda\nabla T)+\nabla\bullet(U\bullet\tau)+U\bullet S_M+S_E\text{............(3)}$$

To describe turbulence and its effects on flows in the HSBD, the standard turbulence model was adopted in this study since it is the most widely applied turbulence model to practical engineering flows as it is robust, economical and provides reasonable accuracy for a wide range of flows.

The turbulence model assumes conservation of turbulence kinetic energy, *k*, and its corresponding dissipation rate ε, through the following relations:

$$\frac{\partial(\rho k)}{\partial t}+\nabla\bullet(\rho U k)=\nabla\bullet\left[\left(\mu+\frac{\mu_t}{\sigma_k}\right)\nabla k\right]+P_k-\rho\varepsilon\text{...(4)}$$

$$\frac{\partial(\rho\varepsilon)}{\partial t}+\nabla\bullet(\rho U\varepsilon)=\nabla\bullet\left[\left(\mu+\frac{\mu_t}{\sigma_\varepsilon}\right)\nabla\varepsilon\right]+\frac{\varepsilon}{k}(C_{\varepsilon 1}P_k-C_{\varepsilon 2}\rho\varepsilon)\text{..(5)}$$

where: $C_{\varepsilon 1}$, $C_{\varepsilon 2}$, σ_k and σ_ε are constants given as 1.44,1.92,1.0 and 1.3 respectively for most computations.

In (1)-(5); ρ is the mass density (Kg/m^3), p is the static pressure (Pa), U is the velocity vector (m/s), S_M is the momentun source (Kg/m^{2}s^2) ; μ is the coeffient of dynamic viscosity (Kg/m/s), the superscript ^{T} denotes the transpose of the tensor, h_{tot} is the specific enthalpy (m^2/s^2]; S_E is the energy source (kg/ms^3); T is the temperatuere (*K*) ; λ is the thermal conductivity(Kgm/s^3/K), t is the time (*s*), P_k is the turbulence production due to viscous and bouyancy forces (kg/m/s^3), μ_t is the turbulent viscosity (kg/m/s), ε is the turbulence dissipation rate (m^2/s^3) and k is the turbulence kinetic energy per unit mass (m^2/s^2)

C. Simulation Procedure

a) Geometry

The geometry of the HSBD was created using AutoCAD and then exported to ANSYS Design Modeler software which is specifically designed for the creation and preparation for simulation. The geometry of the HSBD consisted of dryer and collector regions (Fig. 5). Each region was modeled as a fluid domain and then interfaced together using an option of domain interface during simulation. The complete model was then exported to the ANSYS ICEM for mesh development. The mesh density was increased in the region around the wall edges and in the outlet air ducts (turbo ventilator stalk) where large gradients exist. The mesh size was decided after carrying out a preliminary grid independency analysis with different mesh resolutions. The mesh in the regions near walls, edges and at the turbo ventilator stack were refined. Fine mesh size with a total number of 9900 elements and 2567 nodes was used to provide more accurate results (Fig. 6).

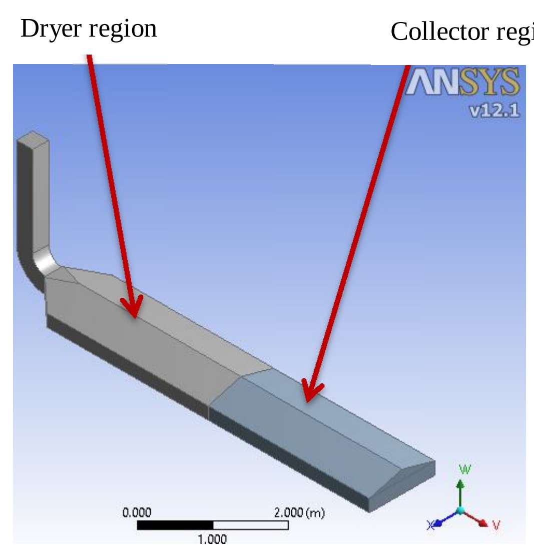

Fig. 1. Geometry of HSBD imported to the design modeler

 ISSN: 2079-6226

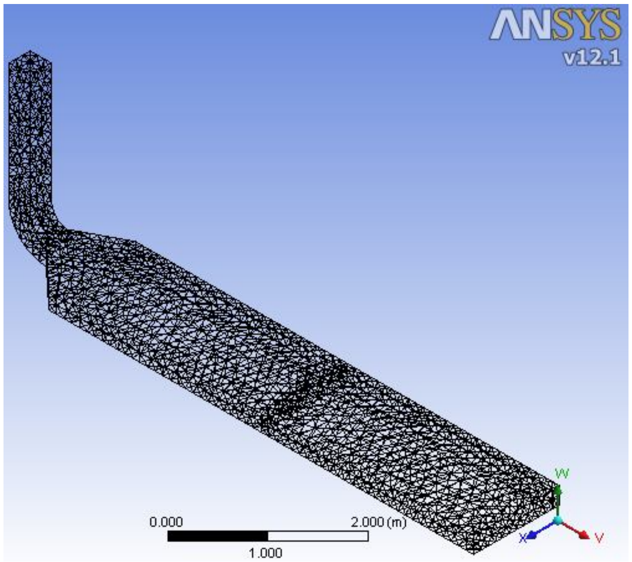

Fig. 2 Mesh from the geometry on ANSYS ICEM CFD

3D simulation analysis was carried out using the commercial CFD package ANSYS CFX 12.1. Model was used to model the effects of turbulence. The physics of the simulation domain was defined in CFX-Pre, the preprocessing module of ANSYS CFX. The two domains were specified as a Non-Buoyant; Stationary Fluid domain with working fluid was assumed as an Ideal gas at 25°C and reference pressure as 1 atm. The ANSYS CFX-Solver module of ANSYS CFX-12.1 was used to obtain the solution of the CFD problem. The solver control parameters were specified in the form of solution scheme and convergence criteria.

Upwind scheme was specified for the solution while for convergence the residual target for RMS values was specified as 10-6. The results were analyzed using CFX-post, the post processor module of ANSYS CFX-12.1.the numerical simulation of the dryer was performed in steady state conditions and then results analyzed.

b) Boundary conditions

The numerical solution of the above equations involves the use of specific boundary conditions, in particular at surfaces bounding of the domain. The set-up of boundary conditions was defined as follows:

Inlet:

The inlet velocity was set at 1 m/s with a turbulent intensity of 5%. The direction of flow was set normal to inlet and temperature of the air assumed to be 70^0C.

Outlet:

A gauge pressure of 0 Pa was assumed at the outlet of the dryer (exhaust stack). The flow regime at both inlet and outlet boundaries was specified as subsonic.

Walls:

At the walls, no slip and smooth wall boundary conditions were used since the velocity near the walls were set at zero. The temperature at the walls was set out considering the measured experimental values and applying a boundary condition of Dirichlet type. At the UV sheet walls, the temperature was set at 55^0C and Monte Carlo technique was used for the additional solar radiation modeling with directional radiation flux of 900 W/m^2. At absorber plate the temperature was also set at 65^0C from the experimental data. The other walls were treated with the default boundary conditions of no slip, with smooth and adiabatic walls due to insulation.

For the necessary turbulent quantities at boundaries the CFX default boundary conditions assumed for each turbulence model were employed. The models constants also were assumed as the default values considered in the CFX code.

III. RESULTS AND DISCUSSIONS

The simulation was done in three dimensions to give the actual and detailed air flow in the dryer, but the results for temperature and velocity profiles were presented in two dimensions since the inlet position is not located at the same plane. The simulation of the dryer was performed without considering the trays and the products to be dried. The model solution in terms of streamlines, contours and vector plots at horizontal and vertical planes in the drying chamber was visualized using ANSYS CFX POST. The criterion of convergence of variables associated with the momentum, heat transfer and turbulence was achieved with 10-4 in conjunction with a maximum of 10 iterations for each time. The convergence associated with the turbulence model was reached at about 10-5, which suggests that the implemented $k-\varepsilon$ model was appropriate. Further, the residuals associated with heat transfer values reached about 10-6, which also suggests that the heat transfer problem was well solved.

Fig. 7 and Fig. 8 shows the temperature distribution in the horizontal plane (at the position of the trays) and vertical plane (mid-section of the dryer) in the HSBD using contour plots respectively. A uniform temperature distribution field was observed along the drying chamber especially in the plane where the tray was fitted. The drying air temperature was between 342.1 K and 356.2 K in the drying chamber, whereas temperatures as high as 384.4 K were observed along the side walls of the dryer. It was observed that the temperature profile of exit air was well developed to affect drying; this indicates that the drying chamber length can be increased and more trays added without any significant drop in the temperature. The uniform temperature profile in the drying chamber could be as a result of additional solar radiation through the UV cover sheet.

ISSN: 2079-6226

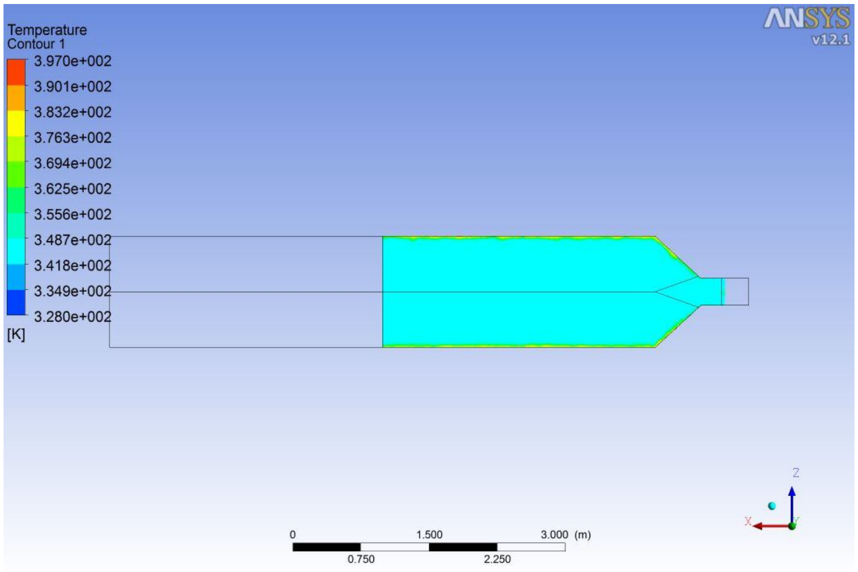

Fig. 3 Temperature distribution in the horizontal plane inside the drying chamber of the HSBD

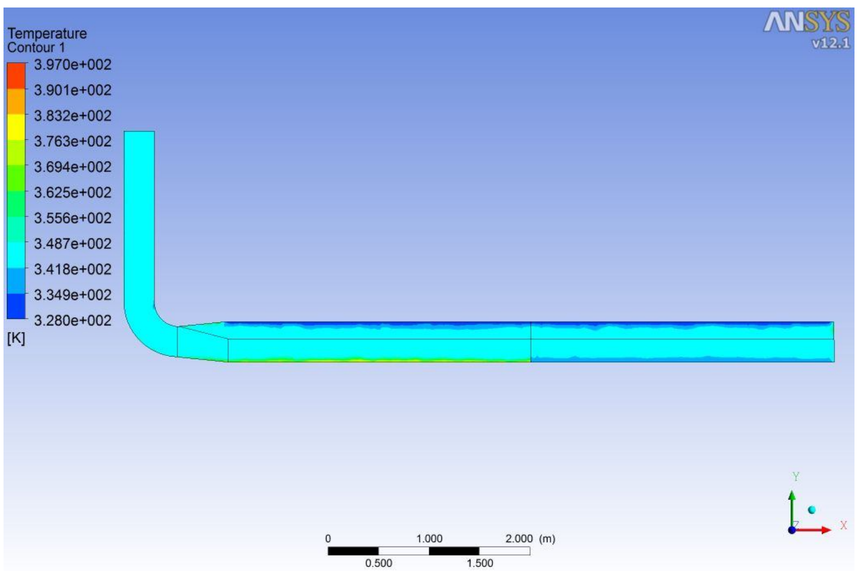

Fig. 4 Temperature distribution in the vertical middle section of the HSBD

Fig. 9 represents the velocity profile of the airflow in the middle section of the HSBD. The maximum air velocity that could be achieved in the drying chamber was 1.55 m/s. The velocity at the inlet as determined by the boundary condition decreased as it entered the solar collector section due to the increased cross sectional area. It was further noted that the velocity was homogeneous at the vertical plane both in the collector and drying chambers. The highest air flow velocity occurred in the exit section of the dryer after it collided with the curved wall. This was due to the reduction in the cross section area as well as the chimney effect; hence the turbulent flows under the convection heat transfer occurred in the exhaust stack because it was in the high air flow region.

 ISSN: 2079-6226

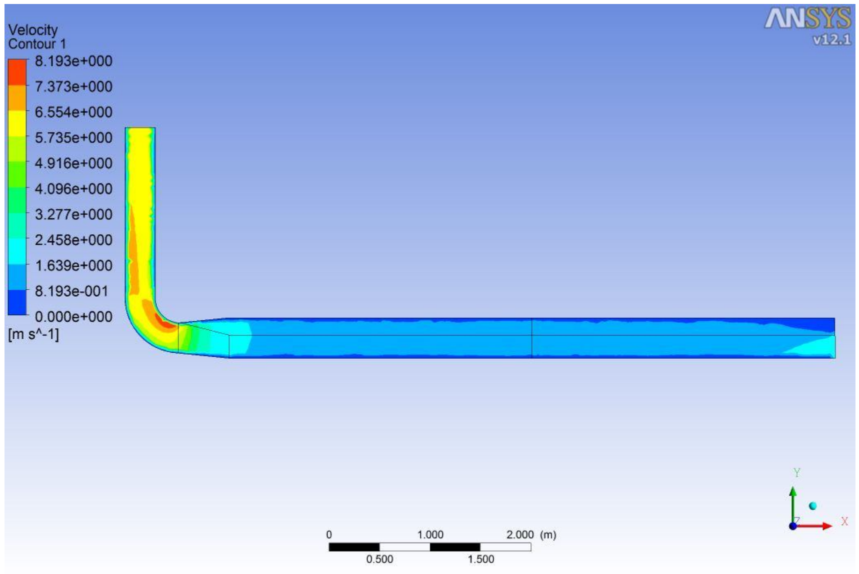

Fig. 5 Velocity profile of airflow in the vertical middle section of the HSBD

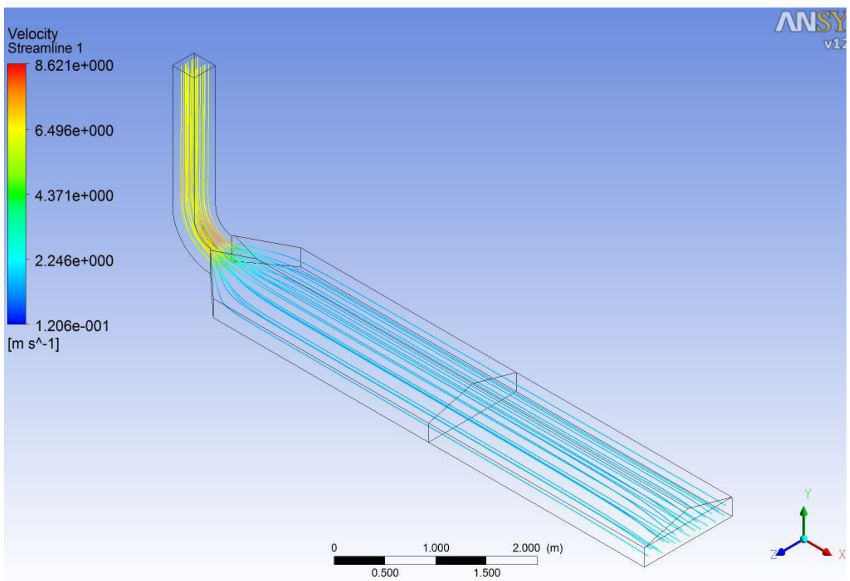

Fig. 6. 3D streamline of airflow inside the HSBD

The simulation result of 3D streamline of airflow in HSBD is as shown in Fig. 10. Streamlines show the movement pattern of the air particles inside the dryer. The streamline pattern inside the dryer showed a smooth and interrupted air flow from inlet section to the exit section of the HSBD. Based on the streamline colour it can be noted that high air velocity was observed at the air exhaust stack. A uniform airflow was also observed throughout the dryer.

 ISSN: 2079-6226

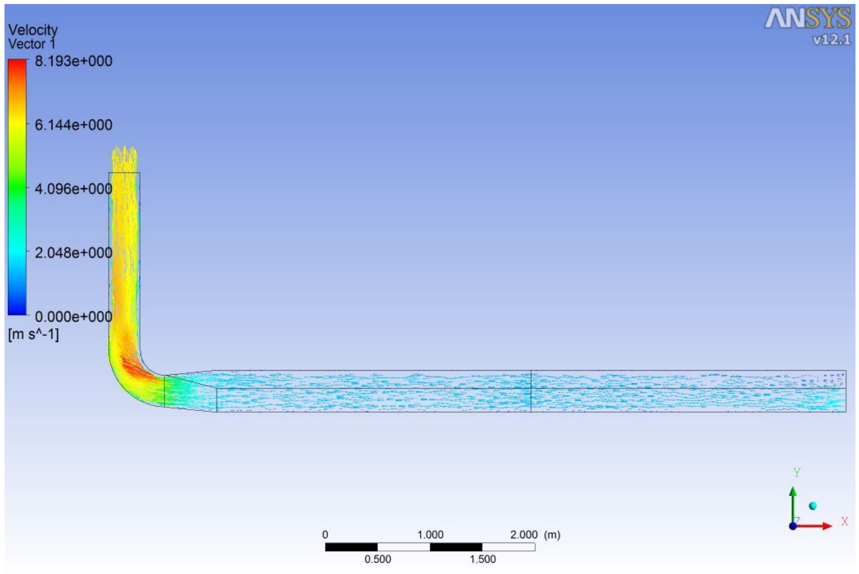

Fig. 7 Velocity vector plot at the vertical middle section of the dryer

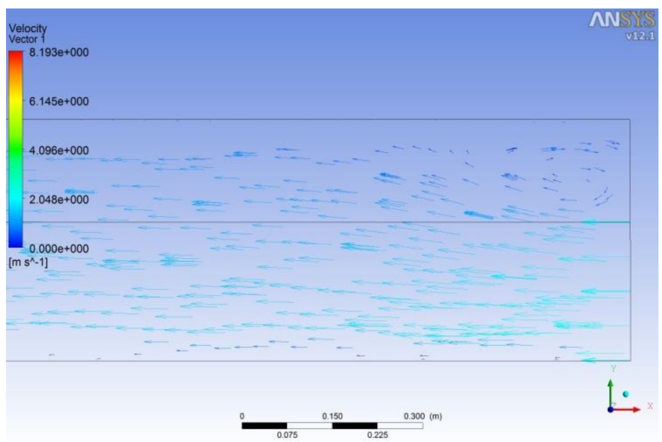

Fig. 8 Velocity vector plot showing recirculation of air in the dryer

Fig. 11 shows the velocity vector plot in the vertical plane at the middle section of the HSBD Velocity vector plots are observed to get the clear picture of flow inside the dryer. The velocity vector plot also reflects whether the separation of flow and recirculation occurs or not. The velocity vector plot was nearly uniform in all the chambers but there was small recirculation of air at the inlet towards the top of the dryer (Fig. 12). The velocity vector plot was concentrated in the central region of both the collector and the drying chamber and less concentrated near the walls. This behaviour of the velocity vector plot is desirable for drying purposes.

IV. Conclusion

Hybrid solar dryers have proven to be successful in drying most agricultural produce. The additional biomass stove- heat exchanger system allows the continuous drying process at night and during wet seasons. This shortens the drying time and improves the quality of product to be dried. CFD simulation is useful in predicting air velocity and temperature profiles in a drying chamber. The commercial CFD package ANSYS CFX-12.1 was used to predict the three dimensional flow in the HSBD. Simulation in 3D provides superior results because it represents the actual problem. The result shows uniform temperature distribution of airflow throughout the dryer. The temperature was maintained almost constant from the collector to drying chamber due to additional heating of air by solar radiation through the UV cover sheet. The velocity of airflow was homogeneous throughout the dryer. This behavior is desirable and suitable for dryer purposes, since it guarantees a high-quality product and homogeneous drying process. The prediction of the airflow inside the dryer can assist to design the most suitable geometric configurations of HSBDs and improve the drying process.

 ISSN: 2079-6226

ABBREVIATIONS AND ACRONYMS

CFD	Computational Fluid Dynamics
GI	Galvanized Ironsheet
HSBD	Hybrid Solar Biomass Dryer
UV	Ultra Violet
KIRDI	Kenya Industrial Research and Development Institute

SYMBOLS

$C_{\varepsilon 1}$	Turbulent model constant
$C_{\varepsilon 2}$	Turbulent model constant
h_{tot}	Specific enthalpy [m^2 / s_2]
k	Turbulence kinetic energy per unit mass [m^2 / s^2]
p	Static pressure [Pa]
P_k	Shear production of turbulence [Kg / ms^3]
S_E	Energy source [$Kg / m / s^2$]
S_M	Momentum source [$Kg / m / s^2$]
t	Time [s]
^{T}	Transpose of tensor
T	Temperature [K]
U	Velocity vector [m / s]
λ	Thermal conductivity [W / mK]
μ	Coefficient of dynamic viscosity [$Kg / m / s$]
μ_t	Turbulent viscosity [$Kg / m / s$]
ρ	Mass density [Kg / m^3]
σ_k	Turbulent model constant for k
σ_ε	Turbulent model constant for ε
τ	Stress tensor
ε	Turbulence dissipation rate [m^2 / s^3]

ACKNOWLEDGEMENT

The authors would like to thank Kenya Industrial Research and Development Institute (KIRDI) for sponsoring this work.

REFERENCES

[1] Prasad, J., Vijay, V.K., Tiwari, G.N. and Sorayan, V.P.S. (2006). Study on performance evaluation of hybrid dryer for turmeric (*Curcuma longa* L.) drying at village scale, Journal of Food Engineering, 75: pp. 497-502.

[2] Barnwal, P. and Tiwari, G.N., \Grape drying by using photovoltaic-thermal (pv/t) greenhouse dryer," An Experimental Study, Solar Energy, vol. 82, pp. 1131{1144, 2008.

[3] Bena, B. and Fuller, R.J., \Natural convection solar dryer with biomass back-up heater," Solar Energy, vol. 72, pp. 75 {82, 2002.

[4] Analysis of a Hybrid Solar-Electrical Dryer, 2007.

[5] Weinberg, Z.G., Chen, Y., Finkelman, S., Ashbell, G. and Navarro, S., \The e effect of moisture level on high-moisture maize (zea mays l.) under hermetic storage conditions in vitro studies," Journal of Stored Products Research, vol. 2, pp. 136 {144, 2008.

[6] Ekechukwu, O.V. and Norton, B., \Review of solar energy drying systems ii: an overview of solar drying technology," Energy Conversion and Management, vol. 2, 615 {655, 1999.

[7] Oyekale, K. O., Daniel, I.O., Ajala, M.O. and Sanni, L.O., \Potential longevity of maize seeds under storage in humid tropical seed stores," Nature and Science, vol. 8, 114 {124, 2012.

[8] Tuite, J. and Foster, G.H., \Control of storage diseases of grain," Annual Review of Phytopathology, vol. 1, pp. 343 {366, 1979.

[9] Rashad A. S., Kurt A. R., Carl J. B., Effects of Deterioration Parameters on Storage of Maize, Agricultural and Bio systems Engineering Presentations, Posters and Proceedings.

[10] Aukah, J., Kerich, D. and Ogola, J. (2013). Development of solar biomass hybrid tunnel dryer for drying grains. In: Trends and Opportunities in the Production, Processing and Consumption of Staple Food Crops in Kenya. (Eds). C. Onyango, G. Unbehend and M. Lindhauer. Chapter 11, pp 111-129. . ISBN: 978-3-944331-17-1, TUD Press, Verlag der Wissenschaften GmbH, Dresden, Germany.

[11] Kiranoudis, C.T., Karathanos, V.T. and Markatos, N.C., \Computational uid dy-namics of industrial batch dryers of fruits," Drying Technology, vol. 17(1&2), pp. 1 {25, 1999.

[12] ANSYS - CFX Solver theory guide."